Korean Journal of Radiology

KJR

Check for updates

Thyroid-Associated Orbitopathy: Evaluating Microstructural Changes of Extraocular Muscles and Optic Nerves Using Readout-Segmented Echo-Planar Imaging-Based Diffusion Tensor Imaging

Huan-Huan Chen, MD[1]*, Hao Hu, MD[2]*, Wen Chen, MD[2], Dai Cui, MD, PhD[1], Xiao-Quan Xu, PhD[2], Fei-Yun Wu, MD, PhD[2], Tao Yang, MD, PhD[1]

Departments of [1]Endocrinology and [2]Radiology, The First Affiliated Hospital of Nanjing Medical University, Nanjing, China

Objective: We aimed to investigate the ability of readout-segmented echo-planar imaging (rs-EPI)-based diffusion tensor imaging (DTI) in assessing the microstructural change of extraocular muscles (EOMs) and optic nerves in patients with thyroid-associated orbitopathy (TAO) as well as in evaluating disease activity.
Materials and Methods: We enrolled 35 TAO patients and 22 healthy controls (HCs) who underwent pre-treatment rs-EPI-based DTI. Mean, axial, and radial diffusivity (MD, AD, and RD) and fractional anisotropy (FA) of the medial and lateral EOMs and optic nerve for each orbit were calculated and compared between TAO and HC groups and between active and inactive TAO groups. Factors such as age, sex, disease duration, mediation, and smoking history between groups were also compared. Logistic regression analysis was used to evaluate the predictive value of significant variables for disease activity.
Results: Disease duration was significantly shorter in active TAOs than in inactive ones ($p < 0.001$). TAO patients showed significantly lower FA and higher MD, AD, and RD than HCs for both medial and lateral EOMs ($p < 0.001$), but not the AD value of lateral EOMs ($p = 0.619$). Active patients had significantly higher FA, MD, and AD than inactive patients for medial EOMs ($p < 0.005$), whereas only FA differed significantly in the lateral EOMs ($p = 0.018$). The MD, AD, and RD of optic nerves were significantly lower in TAO patients than HCs ($p < 0.05$), except for FA ($p = 0.129$). Multivariate analysis showed that the MD of medial EOMs and disease duration were significant predictors for disease activity. The combination of these two parameters showed optimal diagnostic efficiency for disease activity (area under the curve, 0.855; sensitivity, 68.4%; specificity, 96.9%).
Conclusion: rs-EPI-based DTI is promising in assessing microstructural changes of EOMs and optic nerves and can help to indicate the disease activity of TAO, especially through the MD of medial EOMs.
Keywords: *Thyroid-associated orbitopathy; Extraocular muscle; Optic nerve; Diffusion tensor imaging; Readout-segmented echo-planar imaging*

INTRODUCTION

Thyroid-associated orbitopathy (TAO), also known as Graves' ophthalmopathy, is one of the most common autoimmune inflammatory orbital diseases (1, 2). Expansion of extraocular muscles (EOMs) and orbital fat is the most prominent finding, and is responsible for various clinical symptoms, such as proptosis, diplopia,

and restricted eye movement (1, 3, 4). Furthermore, the crowding of orbital tissues at the orbital apex as well as increased retrobulbar pressure and optic nerve stretching could result in compressive optic neuropathy, which is the most serious ophthalmic complication of TAO (4, 5). The disease process can be divided into two distinct phases: the active inflammatory phase and the inactive fibrotic phase. Treatment strategies differ significantly between the two phases. Active inflammatory disease is usually considered to be sensitive to anti-inflammatory treatments, while only surgical treatment can rescue the inactive fibrotic disease (1, 3).

Recently, magnetic resonance imaging (MRI) techniques have been increasingly applied in evaluating TAO by virtue of its superior soft tissue contrast with no ionizing radiation (6-8). Thickness or volume measurements of orbital tissues can help with inspecting the degree of involvement of TAO and can improve diagnostic accuracy (6, 7). Signal intensity on T2-weighted images and contrast-enhanced images can assist in staging and deciding treatment (8). However, the overall accuracy for disease staging is still limited from 55.6% to 71.2% (6-9).

Diffusion tensor imaging (DTI), which provides quantitative information about the microstructural integrities of highly oriented tissues, has been increasingly applied for assessing various orbital diseases, such as glaucoma, optic neuritis, and others (10-13). However, studies that apply DTI to assess microstructural changes in TAO patients are still limited (14, 15), with only two small sample studies (with 20 TAO cases) focusing on EOMs and optic nerves, respectively. Moreover, in previous studies, single-shot echo-planar imaging (ss-EPI) sequences were commonly used for obtaining orbital DTI (11-15). However, ss-EPI is apt to susceptibility artifacts, such as signal-intensity drop-out, geometric distortion, and overall T2*-induced image blurring, especially in poor magnetic field homogeneity and high field strengths (16). As a potential alternative, readout-segmented EPI (rs-EPI, developed by Porter & Mueller (17)), where k-space is divided into a few, segments along the readout direction, has attracted more attention. It has been proven to be useful for improving image quality along with superior normal anatomical structure distinction, compared to ss-EPI (16, 18). To our knowledge, no studies have specifically applied rs-EPI-based DTI in the evaluation of TAO until now.

Therefore, our study aims to investigate the ability of rs-EPI-based DTI in assessing microstructural changes of EOMs

and optic nerves in TAO patients as well as in evaluating disease activity.

MATERIALS AND METHODS

Patient Population

This study was approved by our Institutional Review Board and the informed consent requirement was waived due to its retrospective nature. From February 2017 to December 2017, 35 consecutive TAO patients who underwent orbital MRI for pre-treatment assessment were enrolled in this study. TAO was clinically diagnosed if eyelid retraction occurred in association with objective evidence of thyroid dysfunction or abnormal regulation, exophthalmos, optic nerve dysfunction, or EOM involvement. If eyelid retraction was absent, thyroid dysfunction associated with exophthalmos, optic nerve dysfunction, or EOM involvement was adopted (19). Patients who had undergone radiotherapy and surgical decompression or had inadequate image quality were excluded.

Disease activity was assessed based on the modified 7-point clinical activity score (CAS) (20) and determined for each eye. The eye was considered in the active phase when CAS ≥ 3 and was otherwise classified into the inactive phase. A total of 38 eyes were defined as active and 32 as inactive. Disease severity was assessed by using the modified 17-point NOSPECS classification (20). Three categories were defined as follows: mild (score from 0 to 3), moderate (4 to 7), and severe (8 to 17). Fifty eyes were classified as moderate, followed by twelve mild and eight severe. No patients were diagnosed with dysthyroid optic neuropathy. Additionally, 22 healthy subjects were enrolled and underwent the same MRI protocol.

Magnetic Resonance Examination

Magnent resonance (MR) scans were performed on a 3T MR scanner (Skyra, Siemens Healthineers, Erlangen, Germany) with a 20-channel head coil. Each person was instructed to look at a fixed site with both eyes closed to reduce motion-related errors. DTI was acquired on an oblique axial plane using an rs-EPI sequence. The imaging parameters were as follows: repetition time (TR)/echo time (TE), 2000/83 msec; field of view (FOV), 220 mm; matrix, 190 x 171; slice thickness, 3 mm; slice number, 10; readout segments, 5; non-collinear gradient encoding directions, 30; b = 0 and 1000 s/mm^2. The total imaging time was 5 minutes and 34 seconds.

Conventional imaging protocols included axial T1-weighted imaging (TR/TE, 635/6.7 msec), and axial, coronal, and sagittal T2-weighted imaging (TR/TE, 4000/75–117 msec) with fat suppression. Other parameters were as follows: FOV, 200 mm; matrix, 320 x 320; slice thickness, 3 mm.

Imaging Processing

rs-EPI-based DTI images were postprocessed using DSI Studio software (http://dsi-studio.labsolver.org). The 'DTI' reconstruction method was used to model the eigenvectors, and pixel-by-pixel maps of fractional anisotropy (FA), mean diffusivity (MD), axial diffusivity (AD), and radial diffusivity (RD) were then automatically obtained. For placing regions of interest (ROIs) on the EOMs, polygonal ROIs were manually drawn on all consecutive axial slices including the medial and lateral EOMs in each orbit, avoiding the surrounding fatty tissue. We followed a similar method with the optic nerve and carefully positioned polygonal ROIs at the level of the intra-orbital optic nerve (Fig. 1).

All ROIs were drawn independently by 2 neuroradiologists (reader 1: 8 years of experience; reader 2: 4 years of experience) who were blinded to the clinical condition and study design. The measurements of the two readers were used to calculate the inter-observer reproducibility. Additionally, to assess intra-observer reproducibility, reader 1 re-assessed all the DTI images, spaced at least 1 month apart. The average of the two measurements of reader 1 was applied into the statistical analysis.

Statistical Analysis

All numeric data were averaged and reported as the mean ± standard deviation. The chi-squared test was applied to compare differences between sex, medication, smoking history, and disease severity categories between groups. The independent-samples t test was used to compare differences between age, disease duration, and rs-EPI-based DTI parameters of the medial and lateral EOMs as well as the optic nerve between groups. Multivariate logistic regression analysis was used to evaluate the predictive value of significant variables for determining the active phase by using a forced-entry process. The odds ratios and their 95% confidence intervals were calculated. Receiver operating characteristic curve analysis was performed to evaluate the diagnostic efficiency of the identified parameters for the active phase.

Intraclass correlation coefficients (ICC) with 95%
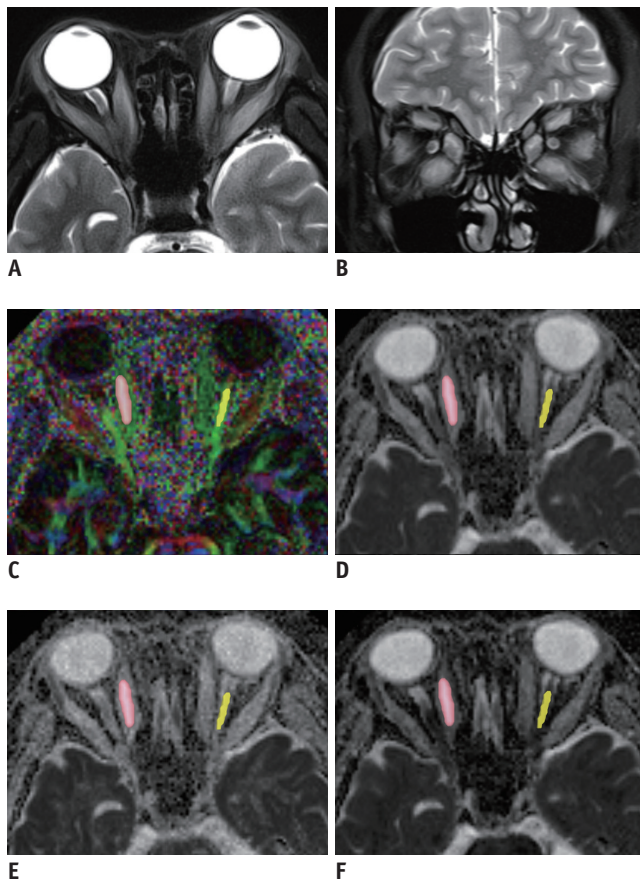
Fig. 1. Methods for measurement of rs-EPI-based DTI parameters in EOMs and optic nerves.
Axial **(A)** and coronal **(B)** fat-suppressed T2-weighted images in 40-year old woman with TAO. Corresponding color-coded FA **(C)**, MD **(D)**, AD **(E)**, and RD **(F)** maps, respectively. Polygonal regions of interest were manually drawn on all consecutive slices of medial and lateral EOMs as well as intra-orbital optic nerve. AD = axial diffusivity, EOM = extraocular muscle, FA = fractional anisotropy, MD = mean diffusivity, RD = radial diffusivity, rs-EPI-based DTI = readout-segmented echo-planar imaging-based diffusion tensor imaging, TAO = thyroid-associated orbitopathy

confidence intervals were used to evaluate the inter- and intra-observer reproducibility of the measurements, and a two-way ICC with random rater assumption was applied. It was interpreted as follows: < 0.40, poor; 0.40–0.60, moderate; 0.61–0.80, good; ≥ 0.81, excellent. A p value of less than 0.05 indicated statistical significance. All statistical analyses were carried out using the SPSS software package (v. 23.0, IBM Corp., Armonk, NY, USA).

RESULTS

Detailed clinical and demographic information of the study population is displayed in Table 1. There were no significant differences in sex distribution or age between

Table 1. Detailed Clinical and Demographic Information of Our Study Population

Variables	TAO (n = 35)			HC (n = 22)	P
	Active	Inactive	P		
Eyes	38	32		44	
Age	47.3 ± 14.9			47.6 ± 14.3	0.822
	48.4 ± 15.9	46.0 ± 13.9	0.367		
Sex (M/F)	14/21			8/14	0.784
	8/11	6/10	0.782		
Disease duration (range)	6.5 ± 4.8 (2–24)				
	4.6 ± 2.3	8.9 ± 5.9	< 0.001*		
Smoking history	7	6	0.968	2	
Antithyroid medication	17	15	0.653	0	
CAS	4.6 ± 1.0	1.3 ± 0.8	< 0.001*		
Modified NOSPECS score	5.2 ± 2.0	5.3 ± 1.3	0.621		
Mild/moderate/severe	10/22/6	2/28/2	0.022*		

Numeric data were reported as mean ± standard deviation. Unit of disease duration is month. *Statistical significance is indicated by *p* values less than 0.05. CAS = clinical activity score, F = female, HC = healthy control, M = male, TAO = thyroid-associated orbitopathy

TAO and healthy control (HC) groups and between active and inactive TAOs, nor were there in antithyroid medication or smoking history between active and inactive TAOs (all *p* > 0.05). The mean disease duration was 6.5 months (range, 2 to 24 months), and it was significantly shorter in active TAOs than inactive ones (4.6 ± 2.3 vs. 8.9 ± 5.9 months, *p* < 0.001). The mean CAS was 4.6 ± 1.0 in active TAOs and 1.3 ± 0.8 in inactive ones (*p* < 0.001). The mean modified NOSPECS score was 5.2 ± 2.0 and 5.3 ± 1.3 in active and inactive TAOs, respectively (*p* = 0.621). A significant difference was found in disease severity categories between active and inactive groups (*p* = 0.022).

Excellent intra- and inter-observer reproducibility were obtained when measuring all rs-EPI-based DTI parameters (ICC ranged from 0.861 to 0.993). TAO patients showed significantly lower FA and higher MD, AD, and RD than HCs (all *p* < 0.001) for both the medial and lateral EOMs, except for the AD value of the lateral EOMs (*p* = 0.619) (Table 2, Fig. 2). Active phase TAO patients had significantly higher FA, MD, and AD (*p* < 0.005) than those in the inactive phase for the medial EOMs, whereas only FA showed a significant difference regarding the lateral EOMs (*p* = 0.018) (Table 3, Fig. 2). In the optic nerve, MD, AD, and RD were significantly lower in TAO patients than HCs (all *p* < 0.05), while FA showed no significant difference (*p* = 0.129) (Table 2, Fig. 3). Neither FA nor diffusivity differed significantly between active and inactive phases (both *p* > 0.05) (Table 3, Fig. 3).

Multivariate analysis showed that the MD of medial EOMs and disease duration were significant indicators for predicting the active phase (*p* = 0.035, 0.010; respectively),

Table 2. rs-EPI-Based DTI Parameters between TAO and HC Groups

Parameters	TAO	HC	P
FA			
Medial EOM	0.423 ± 0.057	0.480 ± 0.045	< 0.001*
Lateral EOM	0.456 ± 0.073	0.527 ± 0.061	< 0.001*
Optic nerve	0.613 ± 0.085	0.593 ± 0.055	0.129
MD			
Medial EOM	1.721 ± 0.175	1.431 ± 0.123	< 0.001*
Lateral EOM	1.808 ± 0.170	1.570 ± 0.198	< 0.001*
Optic nerve	1.315 ± 0.192	1.394 ± 0.124	0.009*
AD			
Medial EOM	2.600 ± 0.255	2.331 ± 0.379	< 0.001*
Lateral EOM	2.809 ± 0.234	2.776 ± 0.396	0.619
Optic nerve	2.326 ± 0.245	2.413 ± 0.172	0.043*
RD			
Medial EOM	1.335 ± 0.176	1.103 ± 0.196	< 0.001*
Lateral EOM	1.359 ± 0.215	1.133 ± 0.193	< 0.001*
Optic nerve	0.809 ± 0.213	0.884 ± 0.143	0.027*

Numeric data were reported as mean ± standard deviation. Units of MD, AD, and RD are x 10^{-3} mm^2/s. *Statistical significance is indicated by *p* values less than 0.05. AD = axial diffusivity, EOM = extraocular muscle, FA = fractional anisotropy, MD = mean diffusivity, RD = radial diffusivity, rs-EPI-based DTI = readout-segmented echo-planar imaging-based diffusion tensor imaging

and the FA of medial EOMs demonstrated a nearly significant result (*p* = 0.05). A higher MD of medial EOMs and shorter disease duration were related to the active phase (β = 10.355, -0.561; respectively). The combination of MD of medial EOMs and disease duration showed optimal diagnostic efficiency for disease activity (area under the curve, 0.855; sensitivity, 68.4%; specificity, 96.9%) (Fig. 4).

Chen et al.
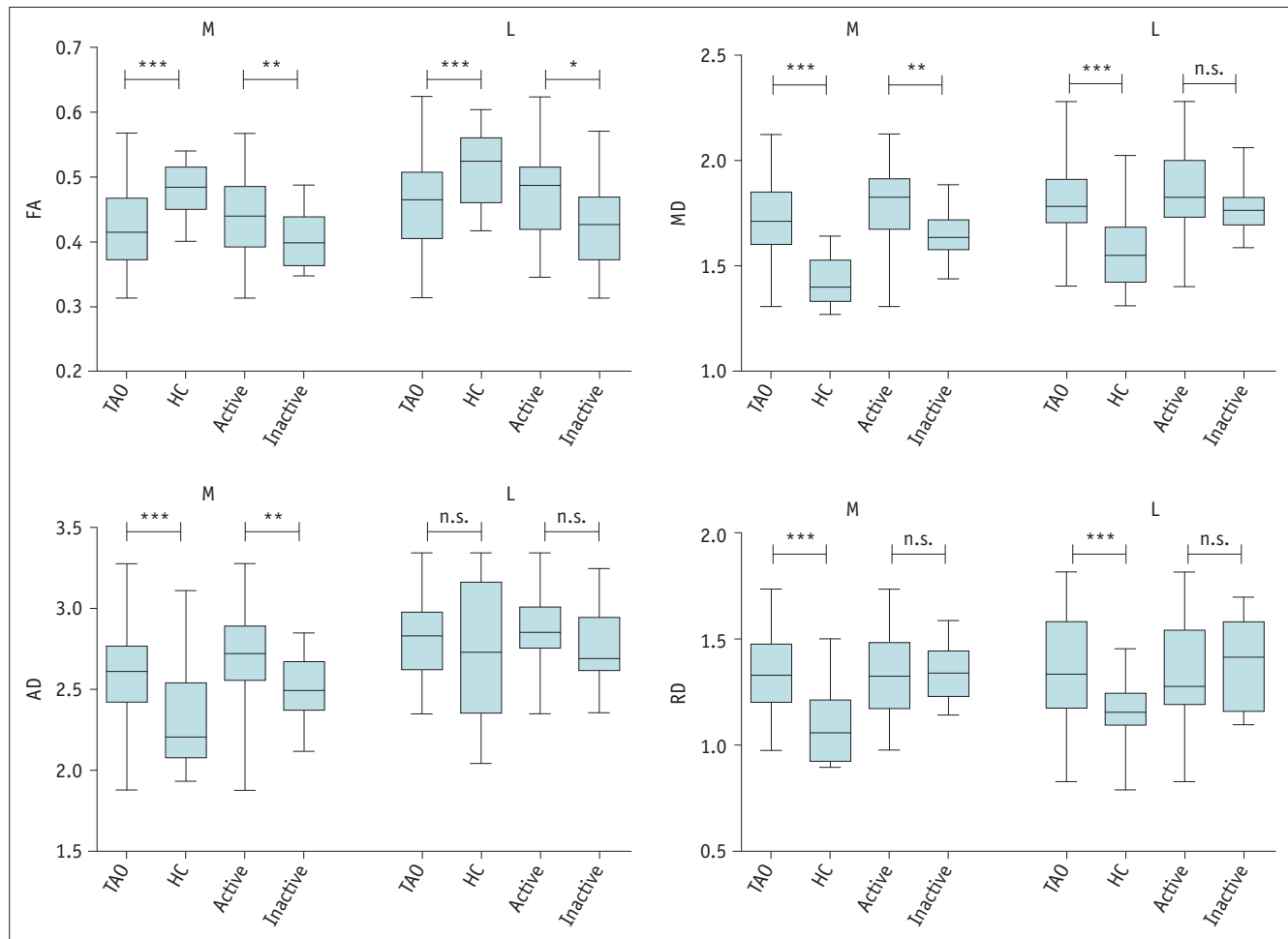
Fig. 2. Box-and-whisker plots show comparisons of all rs-EPI-based DTI parameters in medial and lateral EOMs between groups.
Units of MD, AD, and RD are x 10^{-3} mm^2/s. Asterisk indicates significant difference (***$p < 0.001$, **$p < 0.01$, *$p < 0.05$, n.s. $p > 0.05$). HC = healthy control, L = lateral EOM, M = medial EOM, n.s. = no significance

DISCUSSION

In this study, almost all the diffusivity values of EOMs were significantly higher in TAO patients than those in HCs, which was in agreement with previous studies (21, 22). Furthermore, active patients showed significantly higher diffusivity of medial EOMs than inactive patients. Diffusivity measures the magnitude of diffusion of water molecules within the tissue, which is dominated by interstitial space (23). The active phase is histologically characterized by mononuclear cell infiltration, fibroblast proliferation, and edema in EOMs. By contrast, the inactive phase is characterized by interstitial fibrosis, collagen deposition, and fat infiltration (1, 3). As previous studies stated, diffusivity could increase in edematous muscle and decrease in fibrotic and fatty infiltrated tissue (22-25). Therefore, it is not surprising that active patients have higher

diffusivity than inactive ones. However, this finding might be contradictory to several prior studies (14, 21). Politi et al (21). discovered that the normalized diffusivity of EOMs showed a tendency to increase more in the active phase than in the inactive phase, but this was not statistically significant. In another study, diffusivity values of medial EOMs significantly differed only between acute (disease duration ≤ 6 months) and chronic stages, but not between the active and inactive phases (14). A possible reason for this discrepancy might be the more widened gap of CAS values between active and inactive groups in our study than in the previous two studies. Additionally, the usage of semi-quantitative measurement (diffusivity normalized to thalamus) in the previous study might also have an effect.

FA is another widely used DTI parameter. FA measures the fraction of the magnitude of diffusivity, which reflects fiber integrity and is related to the architecture and the strength
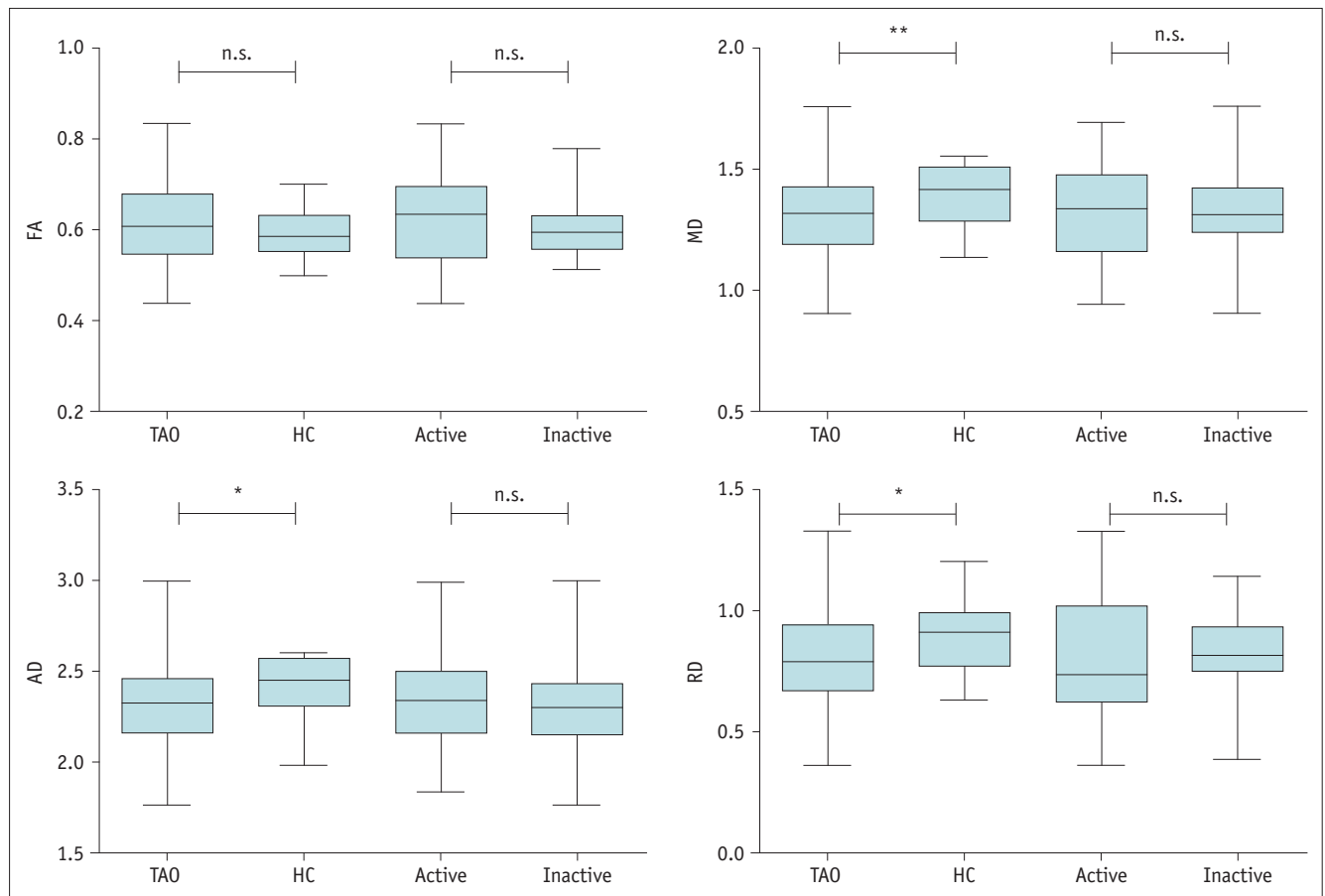
Table 3. rs-EPI-Based DTI Parameters between Active and Inactive Phases

| Parameters	Active	Inactive	P
FA			
Medial EOM	0.440 ± 0.063	0.402 ± 0.043	0.004*
Lateral EOM	0.475 ± 0.072	0.434 ± 0.068	0.018*
Optic nerve	0.622 ± 0.097	0.603 ± 0.067	0.329
MD			
Medial EOM	1.781 ± 0.199	1.648 ± 0.105	0.001*
Lateral EOM	1.840 ± 0.195	1.771 ± 0.127	0.083
Optic nerve	1.316 ± 0.205	1.314 ± 0.179	0.963
AD			
Medial EOM	2.689 ± 0.271	2.493 ± 0.188	0.001*
Lateral EOM	2.859 ± 0.222	2.750 ± 0.237	0.050
Optic nerve	2.349 ± 0.243	2.300 ± 0.250	0.412
RD			
Medial EOM	1.328 ± 0.208	1.343 ± 0.130	0.709
Lateral EOM	1.330 ± 0.230	1.395 ± 0.193	0.210
Optic nerve	0.799 ± 0.243	0.821 ± 0.173	0.674

Numeric data were reported as mean ± standard deviation. Units of MD, AD, and RD are x 10^{-3} mm²/s. *Statistical significance is indicated by p values less than 0.05.

of the muscle (26, 27). In our study, EOMs of TAO patients exhibited lower FA than HCs. This is likely associated with cell lysis, fibrous disruption, or loss of EOMs in TAO patients (14). Furthermore, EOMs of active patients had higher FA values compared to inactive ones, which is a unique finding that has not previously been reported. Previously, Cheung et al (25). discovered decreased FA in mild collagen deposition. Abdullah et al (28). also reported decreased FA in diffuse myocardial fibrosis. Considering that fibrosis and subsequent collagen deposition are also characteristic features of EOMs in inactive TAO, it was not unexpected that inactive patients would show decreased FA compared to active patients.

In our study, multivariate analysis along with clinical factors revealed that MD of medial EOMs and disease duration were significant predictors in combination for disease activity with optimal determining efficiency. In addition, FA of medial EOMs demonstrated a marginal significance in predicting the active phase. Therefore, on the basis of our preliminary results, rs-EPI-based DTI

Fig. 3. Box-and-whisker plots show comparisons of rs-EPI-based DTI parameters in optic nerve between groups. Units of MD, AD, and RD are x 10^{-3} mm²/s. Asterisk indicates significant difference (**$p < 0.01$, *$p < 0.05$, n.s. $p > 0.05$).
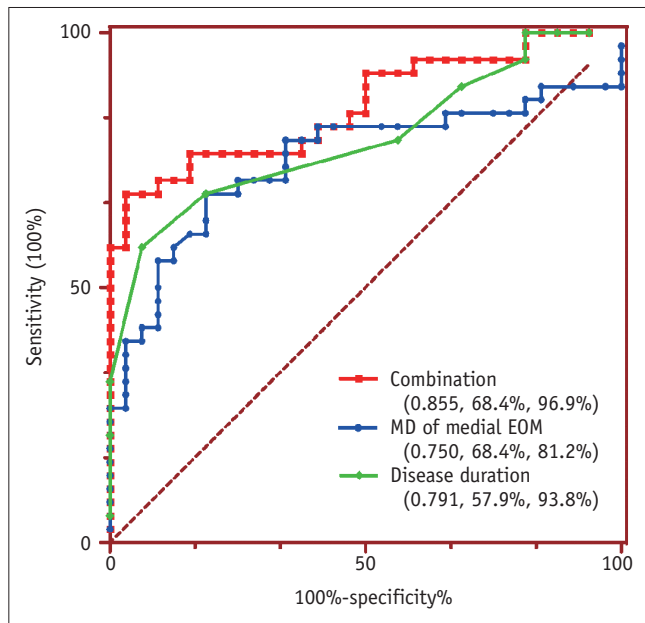
Fig. 4. Receiver operating characteristic curve analysis showed that combination of MD of medial EOMs and disease duration demonstrated optimal diagnostic efficiency for disease activity (area under curve, 0.855; sensitivity, 68.4%; specificity, 96.9%).

derived diffusivity and FA of EOMs, especially of medial EOMs, could be adopted as potential imaging biomarkers for diagnosing TAO and determining activity in patients with TAO.

In terms of microstructural changes in the optic nerve, our study indicated significantly decreased diffusivity in TAO patients compared to HCs, which was consistent with a prior study (15). In addition, Yamada et al (29). found that the diffusivity of the optic chiasm was also decreased significantly in intra- and parasellar tumor patients, and they attributed this change to tumor compression of the optic chiasm starting from the occurrence of the tumor up until treatment. Although the exact mechanisms of dysthyroid optic neuropathy are still not understood, the most widely accepted hypothesis is mechanical compression and ischemia (15). Thus, our present result might also reflect the effects of compression and the relatively long-term change on the optic nerve in TAO patients (29). However, in terms of FA, there is a discrepancy between our study and that of Lee et al (15). They found that FA increased significantly in TAO patients, while our study showed no significance. We thought that this discrepancy might be partially related to the different constitution of patient groups between the two studies. More specifically, patients of a more severe category were included in their

study (20%) compared to ours (11%). In addition, changes in FA values under different scan parameters might also be responsible. For instance, an FA value could be larger when applying a smaller voxel size or decreased diffusion gradient directions (30, 31). Therefore, further research with more unified parameters along with a larger sample size should be performed to clarify the exact change of FA in the optic nerve of patients with TAO.

Our study exhibited good to excellent inter- and intra-observer reproducibility for all measurements of rs-EPI-based DTI parameters. The satisfactory reproducibility might be attributed to the following reasons. First, an rs-EPI sequence was used for the DTI scan. Given that it has been proven to be superior in reducing ghosting artifacts and improving image quality compared to conventional ss-EPI, the better visualization of EOMs and the optic nerve contributes to less measurement bias. Second, as a previous study indicated that inter-observer variability caused by ROI placement could be effectively reduced by a larger ROI approach (32), we used large, polygonal, and strip-like ROIs on consecutive slices, which could objectively represent the overall change of the evaluated subject. By contrast, in previous studies, hot-spot or regional ROIs were usually used for measuring quantitative parameters of EOMs and optic nerves (11, 12, 33). These ROI selection methods were prone to sampling bias.

Our study has several limitations. First, our study population was relatively small. Second, we didn't conduct post-treatment assessment because this is a retrospective study and complete follow-up information was not available for every patient. However, we believe that our results could be a strong basis for further larger prospective studies. Third, while evaluating EOMs, only the medial and lateral bundles were measured because of the axial scan for the DTI sequence. Lack of information on inferior EOMs might be a major drawback of our study. Additional DTI scans in the coronal plane or even using non-EPI diffusion sequences with less air-bone susceptibility artifacts and distortion would be helpful for assessing all EOMs and the optic nerve simultaneously (34, 35).

In conclusion, our preliminary results suggest that rs-EPI-based DTI is helpful in detecting microstructural changes of EOMs and optic nerves and can improve the diagnostic accuracy of TAO. rs-EPI-based FA and diffusivity of EOMs, especially the MD of medial EOMs, can serve as an indicator of disease activity.

ORCID iDs

Tao Yang
  https://orcid.org/0000-0003-1883-4129
Huan-Huan Chen
  https://orcid.org/0000-0003-0201-2059
Hao Hu
  https://orcid.org/0000-0002-7983-7377
Wen Chen
  https://orcid.org/0000-0002-4380-8013
Dai Cui
  https://orcid.org/0000-0003-0356-3362
Xiao-Quan Xu
  https://orcid.org/0000-0001-5493-5256
Fei-Yun Wu
  https://orcid.org/0000-0002-3479-369X

REFERENCES

1. Ludgate M, Baker G. Unlocking the immunological mechanisms of orbital inflammation in thyroid eye disease. *Clin Exp Immunol* 2002;127:193-198
2. Carlé A, Pedersen IB, Knudsen N, Perrild H, Ovesen L, Rasmussen LB, et al. Epidemiology of subtypes of hyperthyroidism in Denmark: a population-based study. *Eur J Endocrinol* 2011;164:801-809
3. Bartalena L, Pinchera A, Marcocci C. Management of Graves' ophthalmopathy: reality and perspectives. *Endocr Rev* 2000;21:168-199
4. Blandford AD, Zhang D, Chundury RV, Perry JD. Dysthyroid optic neuropathy: update on pathogenesis, diagnosis, and management. *Expert Rev Ophthalmol* 2017;12:111-121
5. Gonçalves AC, Gebrim EM, Monteiro ML. Imaging studies for diagnosing Graves' orbitopathy and dysthyroid optic neuropathy. *Clinics (Sao Paulo)* 2012;67:1327-1334
6. Rodríguez-González N, Pérez-Rico C, López-Para Giménez R, Arévalo-Serrano J, Del Amo García B, Calzada Domingo L, et al. [Short-tau inversion-recovery (STIR) sequence magnetic resonance imaging evaluation of orbital structures in Graves' orbitopathy]. *Arch Soc Esp Oftalmol* 2011;86:351-357
7. Szucs-Farkas Z, Toth J, Balazs E, Galuska L, Burman KD, Karanyi Z, et al. Using morphologic parameters of extraocular muscles for diagnosis and follow-up of Graves' ophthalmopathy: diameters, areas, or volumes? *AJR Am J Roentgenol* 2002;179:1005-1010
8. Kirsch EC, Kaim AH, De Oliveira MG, von Arx G. Correlation of signal intensity ratio on orbital MRI-TIRM and clinical activity score as a possible predictor of therapy response in Graves' orbitopathy—a pilot study at 1.5 T. *Neuroradiology* 2010;52:91-97
9. Hu H, Xu XQ, Wu FY, Chen HH, Su GY, Shen J, et al. Diagnosis and stage of Graves' ophthalmopathy: efficacy of quantitative measurements of the lacrimal gland based on 3-T magnetic resonance imaging. *Exp Ther Med* 2016;12:725-729
10. Min J, Park M, Choi JW, Jahng GH, Moon WJ. Inter-vendor and inter-session reliability of diffusion tensor imaging: implications for multicenter clinical imaging studies. *Korean J Radiol* 2018;19:777-782
11. Wang MY, Wu K, Xu JM, Dai J, Qin W, Liu J, et al. Quantitative 3-T diffusion tensor imaging in detecting optic nerve degeneration in patients with glaucoma: association with retinal nerve fiber layer thickness and clinical severity. *Neuroradiology* 2013;55:493-498
12. Wang MY, Qi PH, Shi DP. Diffusion tensor imaging of the optic nerve in subacute anterior ischemic optic neuropathy at 3T. *AJNR Am J Neuroradiol* 2011;32:1188-1194
13. van der Walt A, Kolbe SC, Wang YE, Klistorner A, Shuey N, Ahmadi G, et al. Optic nerve diffusion tensor imaging after acute optic neuritis predicts axonal and visual outcomes. *PLoS One* 2013;8:e83825
14. Han JS, Seo HS, Lee YH, Lee H, Suh SI, Jeong EK, et al. Fractional anisotropy and diffusivity changes in thyroid-associated orbitopathy. *Neuroradiology* 2016;58:1189-1196
15. Lee H, Lee YH, Suh SI, Jeong EK, Baek S, Seo HS. Characterizing intraorbital optic nerve changes on diffusion tensor imaging in thyroid eye disease before dysthyroid optic neuropathy. *J Comput Assist Tomogr* 2018;42:293-298
16. Kim YJ, Kim SH, Kang BJ, Park CS, Kim HS, Son YH, et al. Readout-segmented echo-planar imaging in diffusion-weighted MR imaging in breast cancer: comparison with single-shot echo-planar imaging in image quality. *Korean J Radiol* 2014;15:403-410
17. Porter D, Mueller E. *Multi-shot diffusion-weighted EPI with readout mosaic segmentation and 2D navigator correction.* International Society for Magnetic Resonance in Medicine twelfth scientific meeting and exhibition;2004 May 15-21;Kyoto, Japan
18. Xu XQ, Liu J, Hu H, Su GY, Zhang YD, Shi HB, et al. Improve the image quality of orbital 3 T diffusion-weighted magnetic resonance imaging with readout-segmented echo-planar imaging. *Clin Imaging* 2016;40:793-796
19. Bartley GB, Gorman CA. Diagnostic criteria for Graves' ophthalmopathy. *Am J Ophthalmol* 1995;119:792-795
20. Barrio-Barrio J, Sabater AL, Bonet-Farriol E, Velázquez-Villoria Á, Galofré JC. Graves' ophthalmopathy: VISA versus EUGOGO classification, assessment, and management. *J Ophthalmol* 2015;2015:249125
21. Politi LS, Godi C, Cammarata G, Ambrosi A, Iadanza A, Lanzi R, et al. Magnetic resonance imaging with diffusion-weighted imaging in the evaluation of thyroid-associated orbitopathy: getting below the tip of the iceberg. *Eur Radiol* 2014;24:1118-1126

22. Kilicarslan R, Alkan A, Ilhan MM, Yetis H, Aralasmak A, Tasan E. Graves' ophthalmopathy: the role of diffusion-weighted imaging in detecting involvement of extraocular muscles in early period of disease. *Br J Radiol* 2015;88:20140677

23. Sotak CH. Nuclear magnetic resonance (NMR) measurement of the apparent diffusion coefficient (ADC) of tissue water and its relationship to cell volume changes in pathological states. *Neurochem Int* 2004;45:569-582

24. Bryant ND, Li K, Does MD, Barnes S, Gochberg DF, Yankeelov TE, et al. Multi-parametric MRI characterization of inflammation in murine skeletal muscle. *NMR Biomed* 2014;27:716-725

25. Cheung JS, Fan SJ, Gao DS, Chow AM, Man K, Wu EX. Diffusion tensor imaging of liver fibrosis in an experimental model. *J Magn Reson Imaging* 2010;32:1141-1148

26. Heemskerk AM, Strijkers GJ, Vilanova A, Drost MR, Nicolay K. Determination of mouse skeletal muscle architecture using three-dimensional diffusion tensor imaging. *Magn Reson Med* 2005;53:1333-1340

27. Seo HS, Kim SE, Rose J, Hadley JR, Parker DL, Jeong EK. Diffusion tensor imaging of extraocular muscle using two-dimensional single-shot interleaved multiple inner volume imaging diffusion-weighted EPI at 3 Tesla. *J Magn Reson Imaging* 2013;38:1162-1168

28. Abdullah OM, Drakos SG, Diakos NA, Wever-Pinzon O, Kfoury AG, Stehlik J, et al. Characterization of diffuse fibrosis in the failing human heart via diffusion tensor imaging and quantitative histological validation. *NMR Biomed* 2014;27:1378-1386

29. Yamada H, Yamamoto A, Okada T, Kanagaki M, Fushimi Y, Porter DA, et al. Diffusion tensor imaging of the optic chiasm in patients with intra- or parasellar tumor using readout-segmented echo-planar. *Magn Reson Imaging* 2016;34:654-661

30. Santarelli X, Garbin G, Ukmar M, Longo R. Dependence of the fractional anisotropy in cervical spine from the number of diffusion gradients, repeated acquisition and voxel size. *Magn Reson Imaging* 2010;28:70-76

31. Oouchi H, Yamada K, Sakai K, Kizu O, Kubota T, Ito H, et al. Diffusion anisotropy measurement of brain white matter is affected by voxel size: underestimation occurs in areas with crossing fibers. *AJNR Am J Neuroradiol* 2007;28:1102-1106

32. Wu CJ, Wang Q, Li H, Wang XN, Liu XS, Shi HB, et al. DWI-associated entire-tumor histogram analysis for the differentiation of low-grade prostate cancer from intermediate-high-grade prostate cancer. *Abdom Imaging* 2015;40:3214-3221

33. Özkan B, Anik Y, Katre B, Altintaş Ö, Gençtürk M, Yüksel N. Quantitative assessment of optic nerve with diffusion tensor imaging in patients with thyroid orbitopathy. *Ophthalmic Plast Reconstr Surg* 2015;31:391-395

34. Lingam RK, Mundada P, Lee V. Novel use of non-echo-planar diffusion weighted MRI in monitoring disease activity and treatment response in active Grave's orbitopathy: an initial observational cohort study. *Orbit* 2018;37:325-330

35. Paul K, Graessl A, Rieger J, Lysiak D, Huelnhagen T, Winter L, et al. Diffusion-sensitized ophthalmic magnetic resonance imaging free of geometric distortion at 3.0 and 7.0 T: a feasibility study in healthy subjects and patients with intraocular masses. *Invest Radiol* 2015;50:309-321